Progress In Electromagnetics Research, PIER 90, 323–339, 2009

ANALYSIS OF AN INCLINED SEMI-CIRCULAR SLOT IN THE NARROW WALL OF A RECTANGULAR WAVEGUIDE

A. Ghafoorzadeh and K. Forooraghi

Department of Electrical Engineering
Faculty of Engineering
Tarbiat Modares University (TMU)
Tehran, Iran

Abstract—An inclined semi-circular slot cut in the narrow wall of a rectangular waveguide has been analyzed. By enforcing the boundary condition of continuity of the tangential magnetic field at the slot aperture, an integral equation with the aperture electric field as the unknown has been obtained and solved by the method of moments (MoM). The equivalent slot admittance is then determined. Different slot parameters, such as scattering coefficients, normalized resonant conductance, resonant length versus tilt angle, and radiation patterns, have been studied. The results obtained by the MoM have been verified by comparing them against those results obtained with HFSS.

1. INTRODUCTION

Using the slots in rectangular waveguide walls as radiating elements has become popular since the feed and the radiating structure were integrated in the same waveguide. Also, the insertion loss of such a system is very small. Since the excitation of a radiating slot could be controlled precisely by its physical parameters, an array of slots could be designed to have the desired radiation pattern [1].

Various slots cut on the narrow or broad wall of rectangular waveguides have been studied for a number of years and widely used in radars and satellite systems. Lately, a novel annular waveguide slot antenna (AWSA) has been introduced in [2] and then the derivation of Green's function for AWSA has been presented [3]. Different approaches have been employed for analyzing a slotted waveguide such as those reported in [4, 5]. When the antenna polarization is

Corresponding author: A. Ghafoorzadeh (ghafoorzadeh@modares.ac.ir).

longitudinal (directed along the waveguide) and or the spacing of slots in the planar arrays is less than or equal to one-half wavelength, it is necessary for the slots to be on the narrow wall.

The narrow wall inclined rectilinear slot (edge slot) usually extends to a small region on both broad walls of the rectangular waveguide to produce resonance. The difficulty of modeling the wall thickness region and the complexity of the exterior region of this structure make the edge slot antenna very difficult to analyze. Additionally, fabrication of edge slot planar arrays becomes complicate, since metallic spacers should be placed in between the guides, which in turn increases the backlobe of the planar array.

The edge slots have been investigated with various methods [6–15]. Hashemi-Yeganeh and Elliott [16] analyzed untilted edge slots excited by tilted wires in a rectangular waveguide. They showed that the slots could be in resonance condition while they have not extended into the broad walls. Hirokawa et al. [17] analyzed this structure by including the actual geometry, using a spectrum of the two-dimensional solutions (S2DS) method [18, 19]. Hirokawa and Kildal [20] proposed another excitation technique by inserting a dielectric plate into the slot on which conducting strips were etched. Recently, a linear edge slot array antenna has been analyzed by hybrid finite element-boundary integral (FE-BI) equation method [21].

To overcome the mentioned problems, difficulty of analysis and complexity of fabrication, two compact resonant structures that do not extend into the broad wall, such as C- and I-shaped slots, have been investigated [22, 23]. Also, a dielectric filled inclined edge slot has been reported in order to reduce the resonant length [24]. It should be noted that the C-shaped slot is not symmetrical and its rotation varies the excitation. This rotation shifts the poorly defined phase center of a C-slot and complicates the array design [22]. The resonant conductances of symmetrical I-slots are small compared to the edge slots. Typical resonant slotted arrays require large slot conductance, making the application of I-slot impractical. But traveling-wave arrays use slots with small resonant conductance, which are practical with I-slot [23]. Furthermore, in both I- and C-slots, the aperture electric field distribution is not sinusoidal and varies for different excitations. The use of a dielectric in order to reduce the resonant length decreases frequency bandwidth.

Using a semi-circular slot in the narrow wall of a rectangular waveguide is the main idea of this paper. According to our knowledge, the resulting device has not been studied until now. Therefore its computational analysis is also the new aspect of this paper. In the present work, an inclined semi-circular slot cut in the narrow wall of

a rectangular waveguide is analyzed. The proposed slot fits entirely on the narrow waveguide wall at resonance, which constitutes the main advantage of this slot. In addition, the aperture electric field distribution is sinusoidal at resonance and does not depend on the tilt angle. Also, we show that an inclined semi-circular slot can be modeled by means of shunt admittance and its resonant conductance can be used to design both resonant slotted and traveling-wave arrays.

The analysis method is an entire domain MoM with sinusoidal basis functions for the zero wall thickness structure. Then, we modify our model to account for the finite wall thickness by considering the slot region as a stub waveguide [25]. Results from MoM full-wave analysis and HFSS solution are presented and compared.

It should be noted that the purpose here is to analyze only one semi-circular slot and we intend to investigate a semi-circular slot array in future work. Mutual coupling requires most of the computation time in the analysis or synthesis of the slot arrays. The analysis and computation of mutual coupling has received much attention in the articles, for example in [26] and [27]. In addition, an analysis of mutual coupling has been described for a finite array of different-sized rectangular waveguides arranged on a rectangular grid [28]. In this approach, a formula was derived via Lewin's method that reduces the quadruple integral to four double integral. Mutual coupling for arrays of flange-mounted elliptical waveguides has been evaluated in [29] by the appropriate use of potential and new Green's function expressions in elliptical coordinate that make the significant reduction of the computation time. An analysis of mutual coupling between modes in different-sized coaxial apertures has also been described in [30]. In this approach, the solution is given in terms of Hankel transforms and these are converted to a form suitable for numerical calculation.

2. ANALYSIS

For convenient reference, the geometry of an inclined semi-circular slot cut in the narrow wall of a rectangular waveguide is shown in Fig. 1. The slot is of inner radius r_1, outer radius r_2, width w where $w = r_2 - r_1$, mean length $l_\circ$ where $l_\circ = \pi r_\circ = \pi(r_1 + r_2)/2$, and tilt angle $\theta_\circ$. The center of the semi-circle is on the center of the narrow wall.

We use the cylindrical coordinate in order to formulate the problem. It is defined as follows:

$$\begin{cases} y = b/2 + r\cos\theta \\ z = r\sin\theta \end{cases}$$

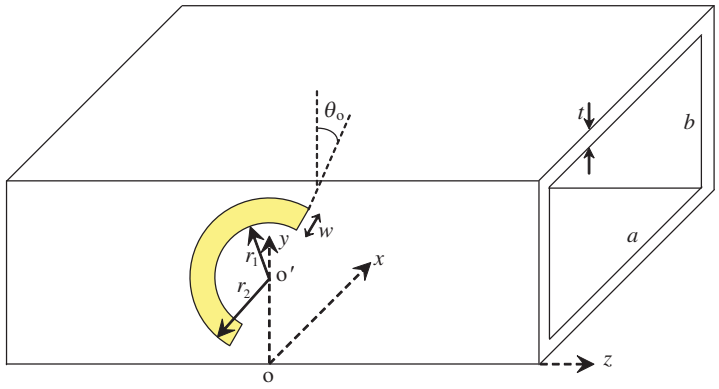

Figure 1. Semi-circular slot in narrow wall of rectangular waveguide.

The transformation of the electric field components from cylindrical to rectangular coordinate is as follows:

$$\begin{cases} E_y(x=0,r,\theta) = \cos\theta E_r(\theta) \\ E_z(x=0,r,\theta) = \sin\theta E_r(\theta) \end{cases}$$

At first, we consider the zero wall thickness ($t = 0$) case. The effect of the finite wall thickness will be accounted later. It is assumed that a TE_{10} mode excites the slot and it is embedded in an infinite ground plane. In addition, we assume that the slot aperture electric field has only a radial component and only depends on the θ variable ($E_{slot} = E_r(\theta)$). This is equivalent to a θ-directed magnetic current on the slot.

According to the geometry, we choose the cylindrical coordinate for simplicity. The procedure that employed to analyze the proposed slot is similar to the one that reported in [24, 25]. Therefore, in order to determine the characteristics of the slot, we have to formulate an integral equation in terms of the unknown electric field in the slot ($E_r(\theta)$). The unknown $E_r(\theta)$ is assumed constant across the slot and is expanded as follows:

$$\overline{E}_{slot} = \hat{r}E_r(\theta) = \hat{r}\sum_{p=1}^{N_s} e_p \sin\left[p(\theta_\circ - \theta)\right]$$
$$r_1 < r < r_2, \quad (-\pi + \theta_\circ) < \theta < \theta_\circ. \tag{1}$$

Thus the magnetic current sheet $\overline{M}$ on the slot aperture is expressed as

$$\overline{M} = -\hat{x} \times \overline{E}_{slot} = -\hat{\theta}E_r(\theta) \tag{2}$$

In the derivation of the integral equation, we impose the continuity of the tangential component of the magnetic fields in the slot aperture:

$$\left[\overline{H}^{ext}\left(-\overline{M}\right)\right]\cdot\hat{\theta}=\left[\overline{H}^{scat}\left(-\overline{M}\right)+\overline{H}^{inc}\right]\cdot\hat{\theta} \tag{3}$$

The details of (3) can be written as

$$H_{\theta}^{ext}\left(-\overline{M}\right)=-\sin\theta H_{y}^{scat}\left(-\overline{M}\right)+\cos\theta H_{z}^{scat}\left(-\overline{M}\right)+\cos\theta H_{z}^{inc} \tag{4}$$

where H_{θ}^{ext} corresponds to the external field that radiates outside the slot, H_{y}^{scat} and H_{z}^{scat} are the internally scattered fields in the waveguide, and H_{z}^{inc} is the incident TE_{10} waveguide field. Using the image principle, one finds that the external magnetic field is given by

$$H_{\theta}^{ext}(r,\theta)=\frac{1}{2\pi j\omega\mu_{\circ}}\int\limits_{slot}E_{r}\left(\theta'\right)\left(k_{\circ}^{2}+\frac{1}{r^{2}}\frac{\partial^{2}}{\partial\theta'^{2}}\right)\frac{e^{-jk_{\circ}R}}{R}r'dr'd\theta' \tag{5}$$

where $k_{\circ}$ is the free space wavenumber and $R=\sqrt{r^{2}+r'^{2}-2rr'\cos(\theta-\theta')}$.

Using Stevenson's Green's functions [6, 31], the internal scattered fields have been derived as follows:

$$\begin{aligned}H_{y}^{scat}(x=0,y,z)=&\frac{2}{j\omega\mu_{0}ab}\sum_{m=0}^{\infty}\sum_{n=0}^{\infty}\frac{\varepsilon_{mn}^{2}}{\gamma_{mn}}\sin\frac{n\pi y}{b}\left\{\left[(k_{0}^{2}-\left(\frac{n\pi}{b}\right)^{2}\right]\right.\\&\cdot\int\limits_{slot}\sin\frac{n\pi y'}{b}E_{z}(0,y',z')e^{-\gamma_{mn}|z-z'|}ds'\\&\left.-\frac{n\pi}{b}\int\limits_{slot}\cos\frac{n\pi y'}{b}E_{y}\left(0,y',z'\right)\frac{\partial}{\partial z'}e^{-\gamma_{mn}|z-z'|}ds'\right\}\end{aligned} \tag{6}$$

and

$$\begin{aligned}H_{z}^{scat}(x=0,y,z)=&\frac{2}{j\omega\mu_{0}ab}\sum_{m=0}^{\infty}\sum_{n=0}^{\infty}\frac{\varepsilon_{mn}^{2}}{\gamma_{mn}}\cos\frac{n\pi y}{b}\\&\cdot\int\limits_{slot}\left\{-E_{y}\left(0,y',z'\right)\cos\frac{n\pi y'}{b}\left[\left(\frac{\partial^{2}}{\partial z'^{2}}+k_{0}^{2}\right)e^{-\gamma_{mn}|z-z'|}\right]\right.\\&\left.-E_{z}(0,y',z')\left(\frac{n\pi}{b}\right)\sin\frac{n\pi y'}{b}\frac{\partial}{\partial z'}e^{-\gamma_{mn}|z-z'|}\right\}ds'\end{aligned} \tag{7}$$

where $y=b/2+r\cos\theta$, $z=r\sin\theta$, $E_{y}=\cos\theta' E_{r}$, $E_{z}=\sin\theta' E_{r}$, $\gamma_{mn}=[(m\pi/a)^{2}+(n\pi/b)^{2}-k_{\circ}^{2}]^{1/2}$, $\varepsilon_{00}^{2}=1/4$, $\varepsilon_{m0}^{2}=1/2$, $\varepsilon_{0n}^{2}=1/2$, and $\varepsilon_{mn}^{2}=1$ if $m\neq 0$ and $n\neq 0$.

The incident H_z^{inc} field is given by $H_z^{inc} = jA_{10}e^{-j\beta_{10}z}$, where A_{10} is the amplitude and β_{10} is the propagation constant of TE_{10} mode. Let $A_{10} = 1$ for convenience. Substituting (5)–(7) in (4) yields an integral equation. The integral equation (4) has been solved by Galerkin's approach of the MoM procedure. For simplicity, the details are omitted here. The resulting matrix can be written as

$$[\mathbf{Y}]_{N\times N}[\mathbf{e}]_{N\times I} = [\mathbf{I}]_{N\times I} \tag{8}$$

where $[\mathbf{e}]$ is a column matrix containing the N_s coefficients of basis functions for $E_r(\theta)$ in (1). A typical element in $[\mathbf{Y}]$ is $y_{pq} = y_{pq}^{ext} + y_{pq}^{int}$, where

$$\begin{aligned} y_{pq}^{ext} &= \int_{-\pi+\theta_\circ}^{\theta_\circ} H_{\theta,p}^{ext}(r = r_\circ, \theta)\sin\left[q(\theta_\circ - \theta)\right] d\theta, \\ y_{pq}^{int} &= \int_{-\pi+\theta_\circ}^{\theta_\circ} -H_{z,p}^{scat}(r = r_\circ, \theta)\cos\theta\sin\left[q(\theta_\circ - \theta)\right] d\theta \\ &\quad + \int_{-\pi+\theta_\circ}^{\theta_\circ} H_{y,p}^{scat}(r = r_\circ, \theta)\sin\theta\sin\left[q(\theta_\circ - \theta)\right] d\theta, \end{aligned}$$

and any source term in $[\mathbf{I}]$ is given by

$$I_q = j\int_{-\pi+\theta_\circ}^{\theta_\circ} e^{-j\beta_{10}r_\circ\sin\theta}\cos\theta\sin\left[q(\theta_\circ - \theta)\right] d\theta.$$

Because of complexity of the matrix elements (y_{pq}), these elements have been necessarily evaluated with numerical analysis. Additionally, due to symmetry, we have been used the fact that $y_{pq} = y_{qp}$ for reducing the computation time.

Once the matrices $[\mathbf{Y}]$ and $[\mathbf{I}]$ are known, the electric field distribution in the slot is obtained easily by solving (8). Then, the dominant mode scattering in the waveguide can be computed using (7) for the TE_{10} mode.

3. FINITE WALL THICKNESS

The waveguide wall thickness can be modeled in a similar manner as derived in [25]. The waveguide wall thickness is accounted for by

introducing higher order waveguide modes in the short stub waveguide connecting the inner and outer regions. Fig. 2 shows a short cylindrical waveguide of semi-circular cross section. The waveguide is of finite length t, inner radius r_1, and outer radius r_2. The waveguide of interest has been analyzed and shown that modes TE_{mn} and TM_{mn} can generally be propagated inside the guide. But, for this special case, the field inside the stub waveguide is described as a superposition of $TE_{m1}\,(m = 1, 2, \ldots)$ modes since the slot width $(w = r_2 - r_1)$ is assumed to be narrow and the variation across the slot is neglected. After analyzing the stub waveguide completely, we have been followed the procedure that employed in [25] for taking into account the waveguide wall thickness effect.

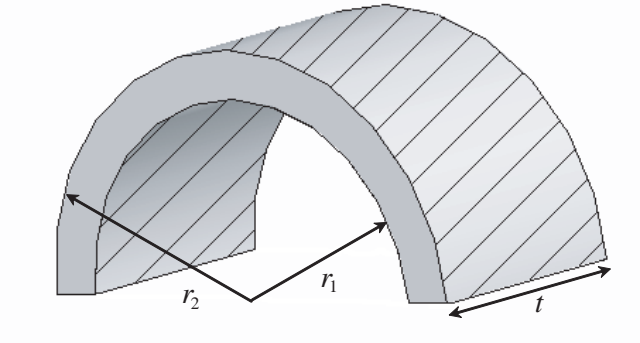

Figure 2. Slot geometry as a short cylindrical waveguide.

4. RESULTS

To study the characteristics of the semi-circular slot, a code has been written using the Matlab software for implementation on a PC Pentium 4 (Intel Core 2 Duo CPU 4400 MHz, 2 GB RAM), based on the employed analysis method. For all of the presented results, the number of ten expansion modes has been considered to determine the slot field in order to achieve sufficient accuracy.

In the numerical computations, the CPU time for one numerical point is about 4 min. Standard X-band WR90 waveguide, slot inner radius $r_1 = 4\,\text{mm}$, slot outer radius $r_2 = 5\,\text{mm}$, and slot inclination angle $\theta_\circ = 30^\circ$ were used in the most of examples.

To validate the present work and computed results, the structure has been simulated using Ansoft HFSS software. Each of points of the HFSS results has been obtained in about 11 min on the used PC

system. Figs. 3 and 4 show a comparison between computed results and those obtained by Ansoft HFSS. These figures illustrate the frequency characteristics of the phase and magnitude of S_{12} in the frequency range 9.5–11.5 GHz. The full-wave analysis and HFSS simulated results can be considered to be in good agreement.

In addition, Fig. 3 presents the computed phase of the slot forward scattering versus frequency for zero waveguide wall thickness case. As mentioned in [32], resonance is defined by the condition that forward scattered TE_{10} mode is out of phase with the incident TE_{10} mode. According to this definition, resonance occurs at frequency where the phase of S_{12} is zero. As observed in Fig. 3, the resonant frequency is 10.5 GHz for zero wall thickness case while resonance occurs at 10.6 GHz for the other case. Fig. 4 also shows the frequency characteristics of the computed magnitude of S_{12} for $t = 0$.

Fig. 5 shows the computed normalized electric field distribution along the slot at resonant frequency (10.6 GHz) for $t = 1.27$ mm waveguide wall thickness. It is noticeable that the slot aperture electric field distribution is nearly a half-cosine distribution.

Now we show that the semi-circular slot in the narrow wall of a rectangular waveguide can be represented by means of a shunt equivalent circuit and in terms of the computed scattering coefficients. For completeness, we use a symmetrical T-network to model the semi-circular slot. The normalized shunt-branch admittance and

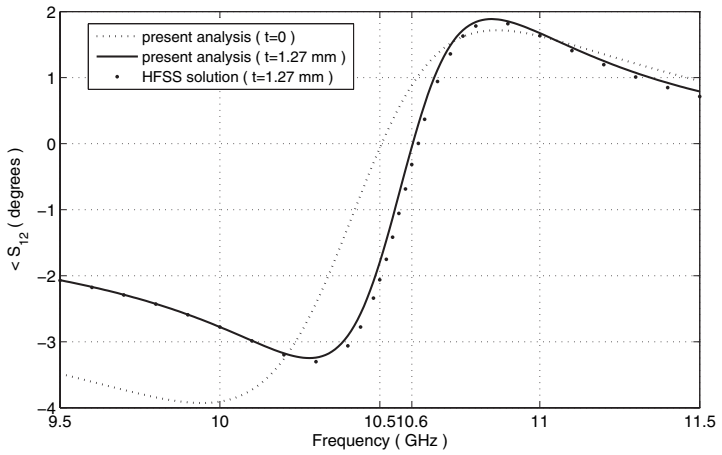

Figure 3. Comparison of HFSS solution and computed phase of S_{12} ($a = 22.86$ mm, $b = 10.16$ mm, $t = 1.27$ mm, $r_1 = 4$ mm, $r_2 = 5$ mm, $\theta_o = 30°$).

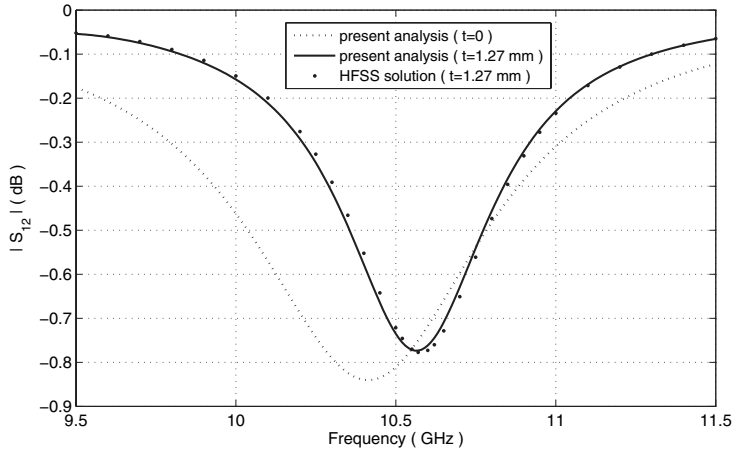

Figure 4. Comparison of HFSS solution and computed magnitude of S_{12} ($a = 22.86\,\text{mm}$, $b = 10.16\,\text{mm}$, $t = 1.27\,\text{mm}$, $r_1 = 4\,\text{mm}$, $r_2 = 5\,\text{mm}$, $\theta_o = 30^\circ$).

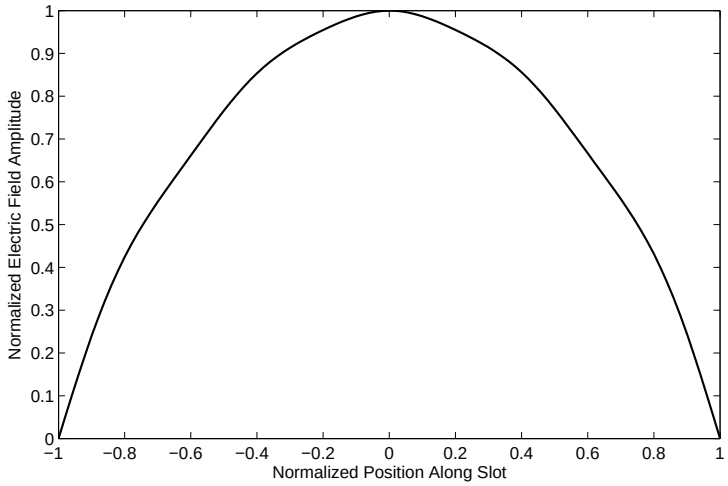

Figure 5. Slot aperture electric field distribution ($a = 22.86\,\text{mm}$, $b = 10.16\,\text{mm}$, $t = 1.27\,\text{mm}$, $r_1 = 4\,\text{mm}$, $r_2 = 5\,\text{mm}$, $\theta_o = 30^\circ$, $f_r = 10.6\,\text{GHz}$).

series-branch impedance of the T-network in terms of the scattering coefficients are $Y = (1 - S_{11} - S_{12})(1 - S_{11} + S_{12})/(2S_{12})$ and $Z = (1 + S_{11} - S_{12})/(1 - S_{11} + S_{12})$. Additionally, the normalized admittance for a

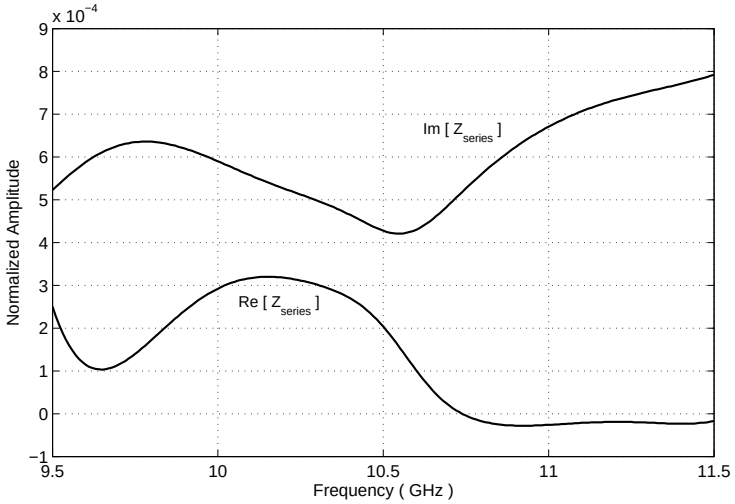

Figure 6. Imaginary and real part of the series-branch impedance of the symmetrical T-network versus frequency ($a = 22.86\,\text{mm}$, $b = 10.16\,\text{mm}$, $t = 1.27\,\text{mm}$, $r_1 = 4\,\text{mm}$, $r_2 = 5\,\text{mm}$, $\theta_\circ = 30^\circ$).

simple shunt model is obtained as $Y/Y_\circ = G + jB = -2S_{11}/(1 + S_{11})$, based on the transmission line theory. Fig. 6 shows the computed normalized amplitude of the imaginary and the real part of the series-branch impedance (Z) versus frequency in the range 9.5–11.5 GHz.

Figure 7 presents a comparison between computed normalized shunt-branch admittance of the symmetrical T-network and computed normalized admittance of a simple shunt model ($Y/Y_\circ = G + jB$). The good agreement is observed. When Figs. 6 and 7 are compared, one can see that the normalized values of the imaginary and real parts of the series-branch impedance are very small such that the T-network model is simplified to a shunt equivalent circuit. Furthermore, the resonant frequency can also be defined, which yields a zero susceptance ($B = 0$). For this example, the resonant frequency is 10.6 GHz. It should be noted, for all computed and simulation results, the phase is referenced to the point where the phase of scattering parameters S_{11} and S_{12} yields to zero together.

Figure 8 shows the normalized resonant conductance versus slot tilt angle at resonant frequency (10.6 GHz) for both semi-circular and edge slots. It compares the computed and HFSS simulated results of the semi-circular slot for validation. Also, it compares the normalized resonant conductance of the semi-circular and edge slots. It is observed that for $\theta_\circ > 11^\circ$ the normalized resonant conductance of the semi-

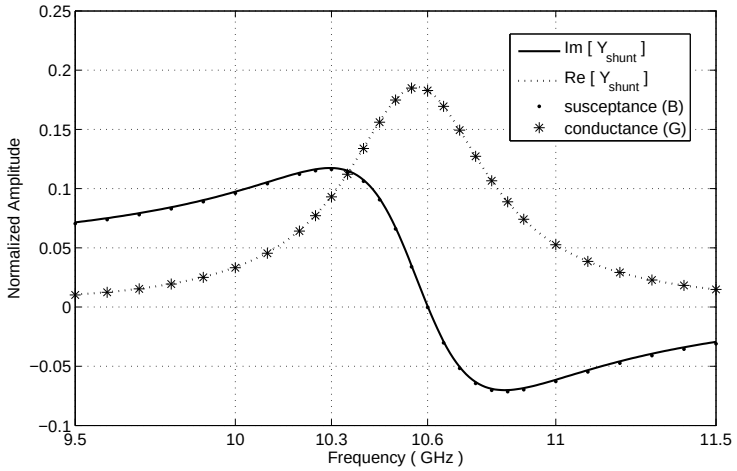

Figure 7. Comparison of shunt-branch admittance of the symmetrical T-network and $Y = -2S_{11}/(1 + S_{11}) = G + jB$ ($a = 22.86\,\text{mm}$, $b = 10.16\,\text{mm}$, $t = 1.27\,\text{mm}$, $r_1 = 4\,\text{mm}$, $r_2 = 5\,\text{mm}$, $\theta_\circ = 30^\circ$).

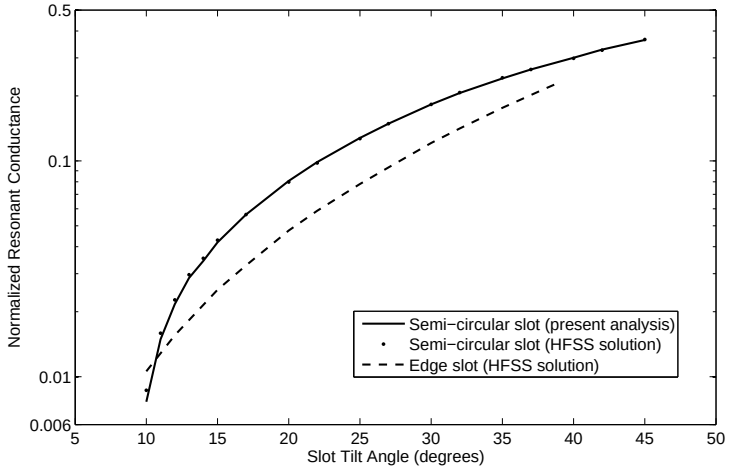

Figure 8. Normalized resonant conductance versus slot tilt angle for two cases, semi-circular slot and edge slot ($a = 22.86\,\text{mm}$, $b = 10.16\,\text{mm}$, $t = 1.27\,\text{mm}$, $w_{\text{edge slot}} = 1\,\text{mm}$, $f_r = 10.6\,\text{GHz}$).

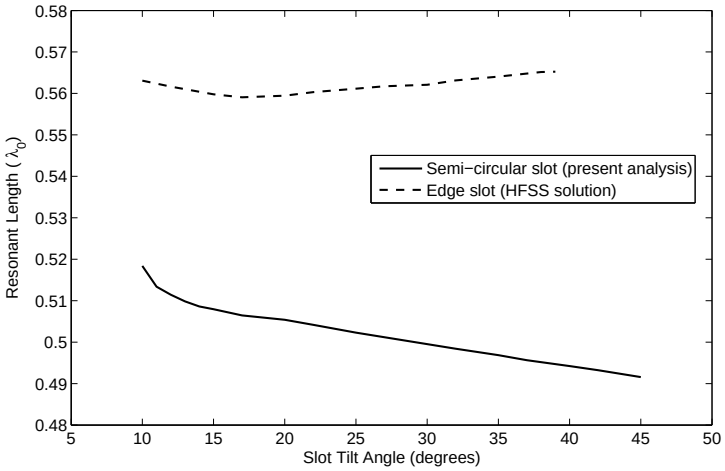

Figure 9. Resonant length versus slot tilt angle for two cases, semi-circular slot and edge slot ($a = 22.86\,\text{mm}$, $b = 10.16\,\text{mm}$, $t = 1.27\,\text{mm}$, $w_{\text{edge slot}} = 1\,\text{mm}$, $f_r = 10.6\,\text{GHz}$).

circular slot is larger than the edge slot. This is one of the advantages of the semi-circular slot with respect to the edge slot. The resonant conductance of the compared slots is very small for $\theta_\circ < 11^\circ$.

Figure 9 compares the computed resonant length of the semi-circular slot and the HFSS simulated resonant length of the edge slot at resonant frequency (10.6 GHz). For semi-circular slot, the slot length, defined mean length of the slot, is $l_\circ = \pi r_\circ = \pi(r_1 + r_2)/2$. For edge slot, the slot length, defined along the center line of the slot, is $L = (b + t)/\cos\theta + 2(\delta - t/2)$ [21]. Delta (δ) is the depth of cut that extends to the waveguide broad walls.

Finally, a comparison between the radiation patterns of the semi-circular slot and the edge slot, in principal E- and H-planes, are shown in Figs. 10 and 11 (magnitude of E_θ as co-polarization and magnitude of E_φ as cross-polarization). The semi-circular slot has $\theta_\circ = 15.2^\circ$ and the tilt angle for edge slot is 25°. To compare the cross-polarization of the semi-circular and the edge slots, they have been designed so that their co-polarization patterns have the same peak level. It should be noted that for the semi-circular slot, peak cross-polarization in E-plane is $-12.4\,\text{dB}$ while for the edge slot is $-5.9\,\text{dB}$. The difference of the amplitudes is 6.5 dB. Again, the cross-polarization in H-plane for the semi-circular slot at $\varphi = 0$ (perpendicular to the slot) is $-12.3\,\text{dB}$ while for the edge slot is $-5.9\,\text{dB}$. In this case, the difference

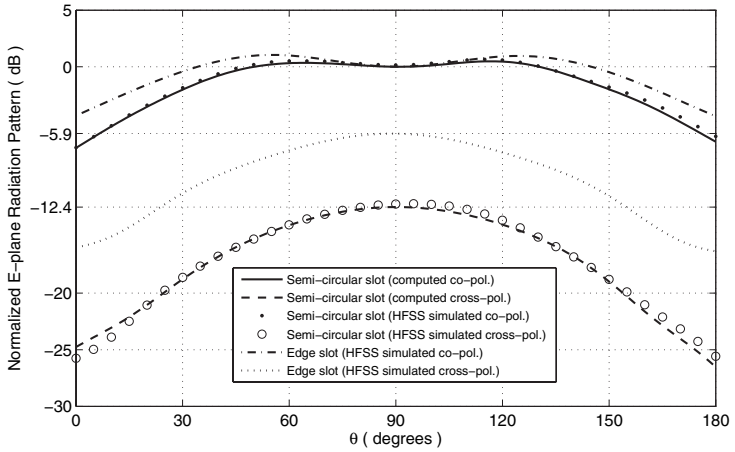

Figure 10. Principal E-plane radiation patterns for two cases, semi-circular slot and edge slot ($a = 22.86\,\text{mm}$, $b = 10.16\,\text{mm}$, $t = 1.27\,\text{mm}$, $f_r = 10.6\,\text{GHz}$, $r_1 = 4.149\,\text{mm}$, $r_2 = 5\,\text{mm}$, $\theta_\circ = 15.2^\circ$, $w_{\text{edge slot}} = 1\,\text{mm}$, $\theta_{\text{edge slot}} = 25^\circ$).

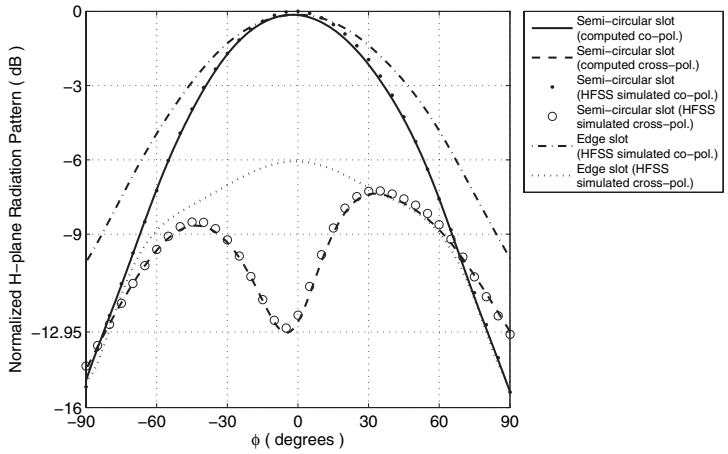

Figure 11. Principal H-plane radiation patterns for two cases, semi-circular slot and edge slot ($a = 22.86\,\text{mm}$, $b = 10.16\,\text{mm}$, $t = 1.27\,\text{mm}$, $f_r = 10.6\,\text{GHz}$, $r_1 = 4.149\,\text{mm}$, $r_2 = 5\,\text{mm}$, $\theta_\circ = 15.2^\circ$, $w_{\text{edge slot}} = 1\,\text{mm}$, $\theta_{\text{edge slot}} = 25^\circ$).

of the amplitudes is 6.4 dB. Therefore, the results show that the cross-polarization of the semi-circular slot is noticeably smaller than the edge slot. This is another advantage of the semi-circular slot with respect to the edge slot.

In addition, Figs. 10 and 11 present a comparison between computed and HFSS simulated radiation patterns for semi-circular slot. As observed in these figures, the computed results are verified with those of obtained by HFSS.

5. CONCLUSION

A novel semi-circular slot cut in the narrow wall of a rectangular waveguide is proposed in this paper. The MoM procedure with entire-domain basis functions has been employed for analyzing the proposed structure. The slot parameters such as normalized resonant conductance and resonant length versus tilt angle and radiation patterns in principal E- and H-planes are presented. To validate the present work, the computed results have been checked with the results obtained by HFSS. A good agreement is observed. The computation time that consumed in the MoM scheme is less compared to HFSS. Therefore, due to the efficiency of this method, calculation of mutual coupling and optimization in array design procedure is practical. To compare the characteristics of the semi-circular slot and edge slot, similar results have been determined by HFSS software for edge slot at required frequency. There are three major advantages for semi-circular slot compared to the edge slot. The semi-circular slot does not extend to the broad wall and fits entirely on the narrow wall. The resonant conductance of the semi-circular slot is larger than the edge slot for $\theta_\circ > 11^\circ$. The cross-polarization of the semi-circular slot is noticeably smaller than the edge slot.

REFERENCES

1. Rengarajan, S. R., L. G. Josefsson, and R. S. Elliott, "Waveguide-fed slot antennas and arrays: A review," *Electromagnetics*, Vol. 19, No. 1, 3–22, 1999.
2. Ebadi, S. and K. Forooraghi, "Comparative study of annular and rectangular waveguides for application in annular waveguide slot antennas (AWSA)," *Journal of Electromagnetic Waves and Applications*, Vol. 22, 2217–2230, 2008.
3. Ebadi, S. and K. Forooraghi, "Green's function derivation of an annular waveguide for application in method of moment analysis

of annular waveguide slot antennas," *Progress In Electromagnetics Research*, PIER 89, 101–119, 2009.

4. Mittra, R. and K. Du, "Characteristics basis function method for iteration-free solution of large method of moments problems," *Progress In Electromagnetics Research B*, Vol. 6, 307–336, 2008.
5. Mondal, M. and A. Chakrabarty, "Resonant length calculation and radiation pattern synthesis of longitudinal slot antenna in rectangular waveguide," *Progress In Electromagnetics Research Letters*, Vol. 3, 187–195, 2008.
6. Stevenson, A. F., "Theory of slots in rectangular waveguides," *Journal of Applied Physics*, Vol. 19, 24–38, 1948.
7. Das, B. N., J. Ramakrishna, and B. K. Sarap, "Resonant conductance of inclined slots in the narrow wall of a rectangular waveguide," *IEEE Trans. Antennas Propag.*, Vol. 32, 759–761, Jul. 1984.
8. Hsu, P. and S. H. Chen, "Admittance and resonant length of inclined slots in the narrow wall of a rectangular waveguide," *IEEE Trans. Antennas Propag.*, Vol. 37, 45–49, Jan. 1989.
9. Raju, G. S. N., A. Chakraborty, and B. N. Das, "Studies on wide inclined slots in the narrow wall of rectangular waveguide," *IEEE Trans. Antennas Propag.*, Vol. 38, 24–29, Jan. 1990.
10. Jan, C. G., P. Hsu, and R.-B. Wu, "Moment method analysis of sidewall inclined slots in rectangular waveguides," *IEEE Trans. Antennas Propag.*, Vol. 39, 68–73, Jan. 1991.
11. Jan, C. G., R.-B. Wu and P. Hsu, "Variational analysis of inclined slots in the narrow wall of a rectangular waveguide," *IEEE Trans. Antennas Propag.*, Vol. 42, 1455–1458, Oct. 1994.
12. Jan, C. G., R.-B. Wu, P. Hsu, and D.-C. chang, "Analysis of edge slots in rectangular waveguide with finite waveguide wall thickness," *IEEE Trans. Antennas Propag.*, Vol. 44, 1120–1126, Aug. 1996.
13. Prakash, V. V. S., S. Christopher, and N. Balakrishnan, "Sidewall inclined slot in a rectangular waveguide: Theory and experiment," *IEE Proc. Microwave Antennas Propagation*, Vol. 145, No. 3, 233–238, Jun. 1998.
14. Prakash, V. V. S., S. Christopher, and N. Balakrishnan, "Method-of-moments analysis of the narrow-wall slot array in a rectangular waveguide," *IEE Proc. Microwave Antennas Propagation*, Vol. 147, No. 3, 242–246, Jun. 2000.
15. Catina, V. and F. Arndt, "Rigorous surface integral method-of-moment analysis of rectangular waveguide edge-slot arrays,"

Antennas and Propagation Society International Symposium, 3145–3148, IEEE, Jul. 2006.

16. Hashemi-Yeganeh, S. and R. S. Elliot, "Analysis of untilted edge slots excited by tilted wires," *IEEE Trans. Antennas Propag.*, Vol. 38, 1737–1745, Nov. 1990.
17. Hirokawa, J., L. Manholm, and P.-S. Kildal, "Analysis of an untilted wire-excited slot in the narrow wall of a rectangular waveguide by including the actual external structure," *IEEE Trans. Antennas Propag.*, Vol. 45, 1038–1044, Jun. 1997.
18. Forooraghi, K. and P.-S. Kildal, "Transverse radiation pattern of a slotted waveguide array radiating between finite height baffles in terms of a spectrum of two-dimensional solutions," *IEE Proc.*, Vol. 140, Pt. H, No. 1, 52–58, Feb. 1993.
19. Forooraghi, K., P.-S. Kildal, and S. R. Rengarajan, "Admittance of an isolated waveguide-fed slot radiating between baffles using a spectrum of two dimensional solutions," *IEEE Trans. Antennas Propag.*, Vol. 41, 422–428, Apr. 1993.
20. Hirokawa, J. and P.-S. Kildal, "Excitation of an untilted narrow-wall slot in a rectangular waveguide by using etched strips on a dielectric plate," *IEEE Trans. Antennas Propag.*, Vol. 45, 1032–1037, Jun. 1997.
21. Young, J. C., J. Hirokawa, and M. Ando, "Analysis of a rectangular waveguide, edge slot array with finite wall thickness," *IEEE Trans. Antennas Propag.*, Vol. 55, 812–819, Mar. 2007.
22. Sphicopoulus, T., "C-slot: A practical solution for phased array of radiating slots located on the narrow side of rectangular waveguides," *IEE Proc.*, Vol. 129, Pt. H, No. 2, 49–55, Apr. 1982.
23. Yee, H. Y. and P. Stellitano, "I-slot characteristics," *IEEE Trans. Antennas Propag.*, Vol. 40, 224–228, Feb. 1992.
24. Heidari, A. A., K. Forooraghi, and M. Hakkak, "Reducing resonant length of sidewall-inclined slots in a rectangular waveguide," *Microwave and Optical Technology Letters*, Vol. 37, 222–226, May 5, 2003.
25. Jossefson, L. G., "Analysis of longitudinal slots in rectangular waveguides," *IEEE Trans. Antennas Propag.*, Vol. 35, 1351–1357, Dec. 1987.
26. Mazzarella, G. and G. Panariello, "On the evaluation of mutual coupling between slots," *IEEE Trans. Antennas Propag.*, Vol. AP-35, 1289–1292, Nov. 1987.
27. Rengarajan, S. R. and E. Gabrelian, "Efficient and accurate evaluation of external mutual coupling between compound broad

wall slots," *IEEE Trans. Antennas Propag.*, Vol. AP-40, 733–737, June 1992.

28. Bird, T. S., "Analysis of mutual coupling in finite arrays of different-sized rectangular waveguides," *IEEE Trans. Antennas Propag.*, Vol. AP-38, 166–172, Feb. 1990.
29. Mongiardo, M. and C. Tomassoni, "Mutual coupling evaluation for arrays of flange-mounted elliptical waveguides," *IEEE Trans. Antennas Propag.*, Vol. AP-49, Issue 5, 763–770, May 2001.
30. Bird, T. S., "Mutual coupling in arrays of coaxial waveguides and horns," *IEEE Trans. Antennas Propag.*, Vol. AP-52, 821–829, March 2004.
31. Elliott, R. S., *An Introduction to Guided Waves and Microwave Circuits*, Ch. 12, Englewood cliffs, Prentice Hall, NJ, 1993.
32. Rengarajan, S. R., "Compound radiating slots in a broad wall of a rectangular waveguide," *IEEE Trans. Antennas Propag.*, Vol. 37, 1116–1123, Sep. 1989.